Chapter 1
Sectional Anatomy of the Thorax

Luciano Alves Favorito and Natasha T. Logsdon

1.1 Introduction

The thoracic cavity is divided into the mediastinum and two pleuropulmonary regions. In this chapter, we will make a brief anatomical description of the organs of the thoracic cavity, and we will show a sequence of transverse cuts of the thoracic cavity demonstrating the relationships between the viscera.

1.2 Mediastinum

The mediastinum is located in the thoracic cavity, being the space between the two pleuropulmonary spaces. It has a large amount of loose connective tissue that surrounds its elements and supports them. With advancing age, this connective tissue becomes more rigid, and the viscera of the mediastinum tend to show less mobility (Netter 1978; Williams et al. 1995).

The limits of the mediastinum are as follows: (1) uppermost—upper opening of the chest, formed by the first two ribs, the manubrium of the sternum and the first thoracic vertebrae; (2) inferior—diaphragm muscle; (3) posterior—thoracic spine;

L. A. Favorito (✉)
Urogenital Research Unit, Rio de Janeiro State University, Rio de Janeiro, RJ, Brazil

IDOMED-UNESA, Rio de Janeiro, RJ, Brazil

The National Council for Scientific and Technological Development (CNPq), Lago Sul, Federal District, Brazil

The Rio de Janeiro State Research Foundation (FAPERJ), Rio de Janeiro, RJ, Brazil

N. T. Logsdon
University Center Geraldo di Biasi, Rio de Janeiro, RJ, Brazil

Urogenital Research Unit, Rio de Janeiro State University, Rio de Janeiro, RJ, Brazil

L. A. Favorito, N. T. Logsdon (eds.), *Atlas of Sectional Anatomy*,
https://doi.org/10.1007/978-3-030-91688-6_1

(4) anterior—posterior surface of the sternum; and (5) lateral—parietal pleura (Testut and Jacob 1926; Williams et al. 1995).

Several diseases (especially tumors and cysts) affect the mediastinum in characteristic locations. Its classic division, in regions, is proposed to facilitate the study of these diseases that affect the mediastinal organs. We can divide the mediastinum into four major regions: upper, anterior, middle, and posterior (Netter 1978).

The upper mediastinum is separated from the other portions by an imaginary line that extends from the sternal angle to the level of the intervertebral disc between the fourth and fifth thoracic vertebrae (Fig. 1.1). This imaginary line passes at the bifurcation of the trachea (called carina), which can also be used as an anatomical point for the division of the mediastinum (Testut and Jacob 1926; Bergman et al. 1988).

The lower part of the mediastinum is divided into three additional portions, using the following parameters: (1) anterior mediastinum—located between the posterior surface of the sternum, anteriorly, and the pericardium, posteriorly; (2) medium mediastinum—located between the two layers of the pericardium; and (3) posterior mediastinum—located between the pericardium, anteriorly, and the spine, posteriorly (Fig. 1.1).

The upper mediastinum contains the esophagus and trachea (posteriorly), the thymus or its remnant (anteriorly), and, in an intermediate position, the great vessels related to the thoracic sympathetic nervous chain of the heart, in addition to the vagus and phrenic nerves (Williams et al. 1995). Several diseases can affect this region of the mediastinum. The most frequent are thymomas, teratomas, plunging goiters (growths of the thyroid gland that reach the chest), adenomegalies, aneurysms, and neurogenic tumors (Nakazono et al. 2019).

The anterior mediastinum has thymus and fatty tissue as its main components (Fig. 1.2). In adults, the thymus and its remnants occupy, preferably, the upper portion of the mediastinum. The main tumors that affect this region are thymomas, lipomas, and teratomas. More rarely, the plunging goiter can reach this location.

The main components of the middle mediastinum are the heart and the immediately adjacent portions of the vessels of the base (Fig. 1.3). Knowledge of cardiac anatomy is very important to radiological image interpretation. Current cardiovascular magnetic resonance (CMR) examinations require expert planning, multiple breath holds, and 2D imaging (Moghari et al. 2020). We must emphasize that when analyzing the sectional images, we must take into account the difference in thickness between the right and left ventricles; as we can see in Figs. 1.3 and 1.4, the left ventricle is approximately the triple in thickness of the right ventricle. The main diseases that can affect this region are pericardial cysts, cardiac tumors, bronchogenic cysts, adenomegalies, teratomas, and lymphangiomas (Nakazono et al. 2019).

In the posterior mediastinum, the esophagus, the descending aorta, the azygos veins, the thoracic duct, lymph nodes, and the thoracic sympathetic chain are located. The commonest termination height of the azygos vein in the superior vein cava (SVC) is at the level of the fifth thoracic vertebrae. The anatomy of the azygos system is of very importance as a predictor for higher values of SVC diameter and mediastinum pathology. Such findings can be useful in mediastinal surgery and mediastinoscopy (Koutsoufianiotis et al. 2021). The main conditions that affect this region are aneurysms, esophageal lesions, bronchogenic cysts, neurogenic tumors, adenomegaly, pheochromocytoma, hiatus hernia, and spinal injuries (Fig. 1.5).

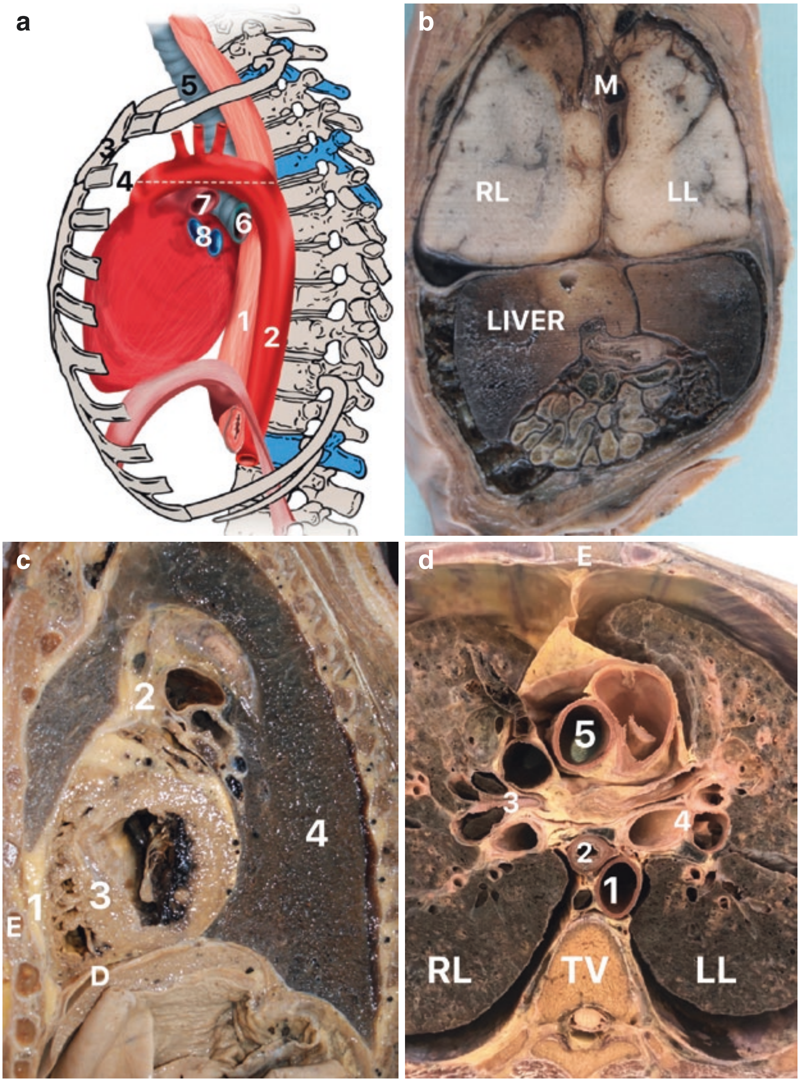

Fig. 1.1 Mediastinum. (**a**) Schematic drawing showing the thoracic cavity and the division of the mediastinum into two compartments by the imaginary line (--------) between the manubrium-sternal junction and the intervertebral body of the fourth thoracic vertebra in superior and inferior mediastinum; 1, esophagus; 2, thoracic aorta artery; 3, sternum; 4, imaginary line that divides the mediastinum; 5, trachea; 6, left main bronchus; 7, left pulmonary artery; 8, left pulmonary vein. (**b**) The figure shows a frontal section in a human frozen fetus in the third gestational trimester showing the relationship between the mediastinum (M) and the right (RL) and left (LL) lungs. (**c**) The figure shows a sagital section of a frozen fresh corpus; we can observe the relationship of the heart (3) with the anterior mediastinal space (1), the lung (4), diaphragm (D), and with the basal vessels (2); E, sternum. (**d**) The figure shows an inferior view of a transverse section of a frozen fresh corpus, at the level of the fourth thoracic vertebra (TV); we can observe some structures of the mediastinum and the relationships with the lungs (RL, right lung; LL, left lung); 1, thoracic aorta artery; 2, esophagus; 3, right pulmonary hilum; 4, left pulmonary hilum; 5, ascending aorta artery

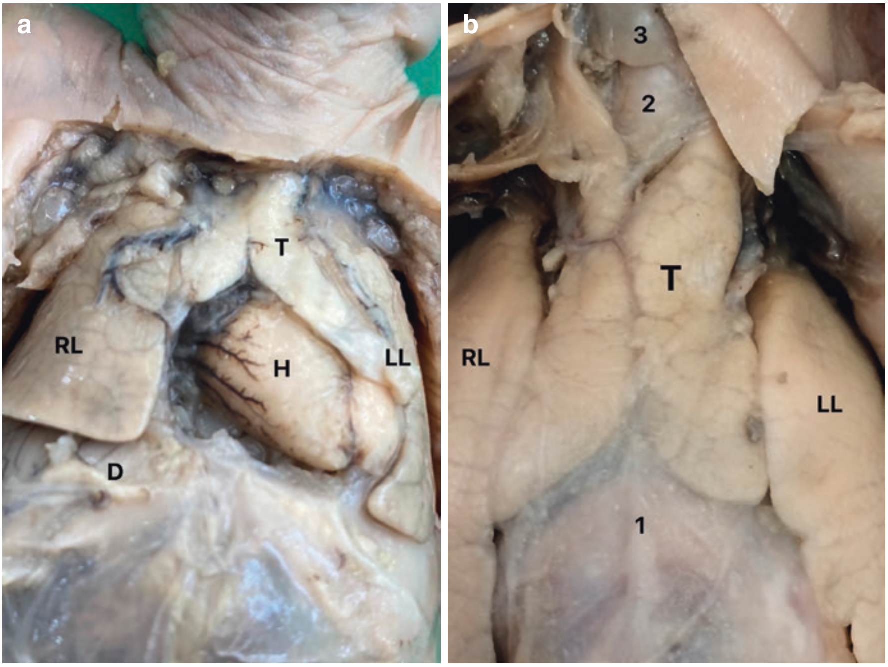

Fig. 1.2 Anterior mediastinum. (**a**) The figure shows the anterior mediastinum of a fixed human fetus in the second gestational trimester; we can observe the timus (T) and the relationships between the heart (H) with the diaphragm (D) and the lungs (RL, right lung; LL, left lung). (**b**) The figure shows the anterior mediastinum of a fixed human fetus in the second gestational trimester; we can observe the timus (T), the pericardium (1), the ascending aorta artery (2), and the tireoid glans (3); RL, right lung; LL, left lung

1.3 Mediastinal Lymph Nodes

Mediastinal lymph nodes can be divided into four main groups: anterior mediastinal, posterior mediastinal, tracheobronchial, and paratracheal (Williams et al. 1995) (Fig. 1.6). Knowledge of their disposition is important due to the diseases that affect them, especially lung cancer.

The posterior mediastinal lymph nodes are located along the esophagus and are responsible for the lymphatic drainage of the intercostal spaces and the parietal pleura. Tracheobronchial lymph nodes are located around the bifurcation of the trachea and along the main bronchi, being divided into the right and left and subcarinal tracheobronchial groups. Subcarinal lymph nodes are of diagnostic importance during the performance of mediastinoscopy and thoracic organ surgeries (Fujiwara et al. 2019). Paratracheal lymph nodes, located along either side of the trachea, drain into the lymph ducts (right and thoracic) and lower cervical lymph nodes (Netter 1978).

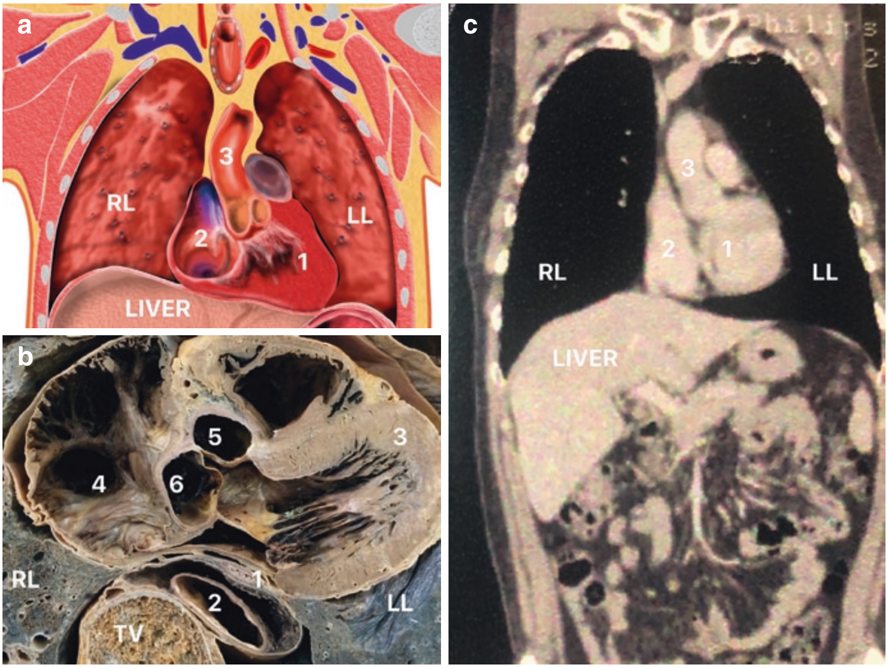

Fig. 1.3 Medium mediastinum. (**a**) Schematic drawing of a frontal section of the thoracic cavity showing some important structures of the medium mediastinum; 1, left ventricle; 2, right atrium; 3, ascending aorta artery; RL, right lung; LL, left lung. (**b**) The figure shows an inferior view of a transverse section of a frozen fresh corpus, at the level of the sixth thoracic vertebra (TV); we can observe some structures of the mediastinum and the relationships with the lungs (RL, right lung; LL, left lung); 1, esophagus; 2, thoracic aorta artery; 3, left ventricle; 4, right ventricle; 5, ascending aorta artery; 6, pulmonary artery. (**c**) The figure shows a thoracic computerized tomography in the frontal section; we can observe the left ventricle (1), the right atrium (2), and the ascending aorta artery (3)

1.4 Pleura and Lungs

1.4.1 Pleura

Pleura is a serous membrane that folds back onto itself to form a two-layered structure that lines the lungs and the inner face of the chest wall. The pleura that surrounds the lungs is called the visceral pleura, and the pleura that is in contact with the chest wall is called the parietal pleura. The two layers are separated by the (virtual) pleural cavity, which is filled with a small amount of pleural fluid. This liquid is essential for sliding between the pleurae and also to prevent the lungs from moving away from the chest wall (Williams et al. 1995).

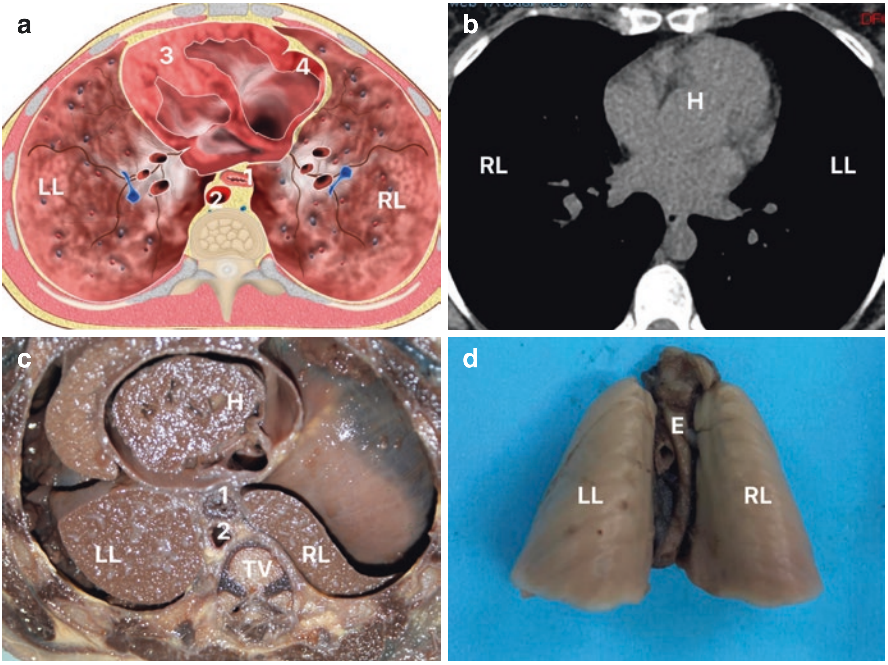

Fig. 1.4 Medium and posterior mediastinum. (**a**) Schematic drawing of a superior view of a transverse section of the thoracic cavity at the level of the sixth thoracic vertebra. We can observe the esophagus (1), the thoracic aorta artery (2), and the relationships between the left ventricle (3) and the right ventricle (4) with the lungs (RL, right lung; LL, left lung). (**b**) The figure shows a thoracic computerized tomography in a transverse section of the thoracic cavity at the level of the sixth thoracic vertebra; we can observe the heart (H) and the lungs (RL, right lung; LL, left lung). (**c**) The figure shows a superior view of a transverse section of the thoracic cavity at the level of the eighth thoracic vertebra. We can observe the esophagus (1), the thoracic aorta artery (2), and the relationships between the heart (H) with the lungs (RL, right lung; LL, left lung). (**d**) In this figure, we can observe the posterior view of thoracic viscera of a human fetus in the second gestational trimester; E, esophagus; LL, left lung; RL, right lung

The visceral pleura follows the divisions of the lungs into lobes, forming pulmonary fissures, and also penetrates the lung parenchyma, dividing the lobes into pulmonary segments. There is no cleavage plane between the visceral pleura and the lung tissue itself. The parietal pleura is separated from the structures of the chest wall by a small amount of connective tissue called endothoracic fascia, and thus the parietal pleura can be easily removed from the chest wall (Netter 1978).

There are four divisions for the parietal pleura according to the area it covers: (1) costal pleura, which lines the ribs and costal cartilages; (2) diaphragmatic pleura, which covers the diaphragm; (3) mediastinal pleura, which is in contact with the mediastinal viscera; and (4) dome of pleura, which lines the pulmonary apex (Mouchova et al. 2018) (Fig. 1.7).

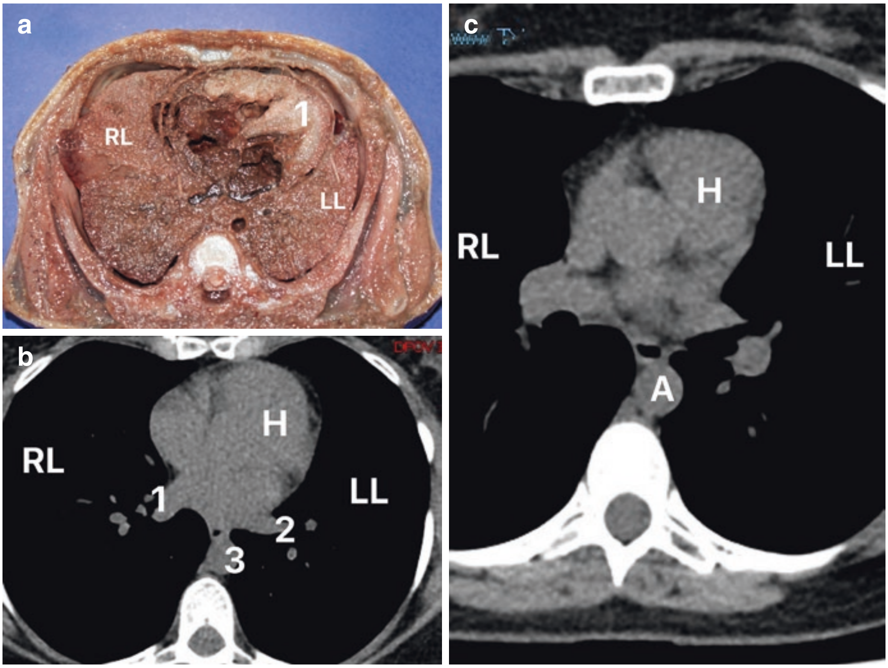

Fig. 1.5 Heart in medium mediastinum. (**a**) The figure shows an inferior view of a transverse section of a frozen fresh fetus in the third gestational trimester at the level of the seventh thoracic vertebra (TV); we can observe the relationships between the heart with the lungs (RL, right lung; LL, left lung). (**b**) The figure shows a thoracic computerized tomography in a transverse section; we can observe the heart (H), left lung (LL), right lung (RL), right pulmonary artery (1), left pulmonary artery (2), and the thoracic aorta artery (3). (**c**) The figure shows a thoracic computerized tomography in a transverse section; we can observe the heart (H), left lung (LL), right lung (RL), and the thoracic aorta artery (A)

The two pleural membranes are continuous in the pulmonary hilum through a pleura cuff that surrounds the structures that enter and leave the lung. Below the root of the lung, the two sides come into contact forming the pulmonary ligament (Williams et al. 1995).

During resting breathing, the expansion of the lungs is not sufficient to fill the entire pleural space. In this way, they form slit-shaped spaces called pleural recesses. There are two pleural recesses: costodiaphragmatic and costomediastinal. The costodiaphragmatic recess is formed between the costal pleura and the diaphragmatic pleura, which are separated only by a capillary layer of pleural fluid. The lower edges of the lungs occupy this space during inhalation; however, on exhalation, the lower edges rise and again allow contact between the two pleural divisions (Fig. 1.8). The same phenomenon is observed in the anterior edges of the lungs that slide in and out of the costomediastinal recesses, during inhalation and exhalation.

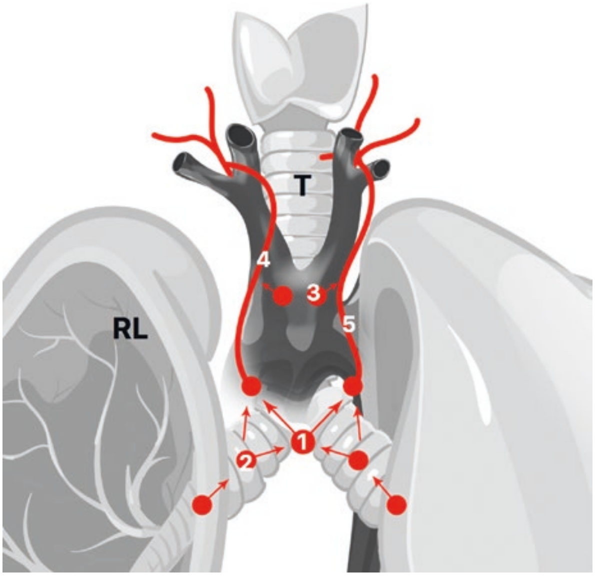

Fig. 1.6 Mediastinal lymph nodes. The figure shows a schematic drawing showing the mediastinal lymph nodes distribution. 1, subcarinal lymph nodes; 2, tracheobronchial lymph nodes; 3, paratracheal lymph nodes; 4, right lymphatic duct; 5, thoracic duct

1.4.2 Lungs

The lungs are conical organs and occupy the lateral regions of the chest cavity from the upper opening of the chest to the diaphragm. However, they are very elastic and reduce their volume to a third or less after opening the chest. They are separated by mediastinal organs such as the trachea, esophagus, heart and major blood vessels (Fig. 1.9).

Each lung has a rounded apex that protrudes into the neck by about 3 cm above the middle part of the clavicle, has a concave base that rests on the diaphragm, and has three faces (costal, diaphragmatic, and mediastinal), which are separated by the anterior margin (separates the mediastinal face from the costal surface anteriorly), posterior margin (separates the mediastinal faces from the costal posteriorly), and inferior margin (separates the diaphragmatic and costal surfaces) (Netter 1978) (Fig. 1.9).

The costal face is large, convex, and related to the costal pleura. The costal face is separated from the ribs, costal cartilages, and intercostal spaces by the costal pleura. The diaphragmatic face is concave and forms the pulmonary base. This concavity is more pronounced in the right lung compared to the left one due to the higher position of the diaphragm on the right because of the liver. The mediastinal face is related to the mediastinal organs, and it is also concave. This concavity is more pronounced on the left, as the heart is shifted two-thirds to the left.

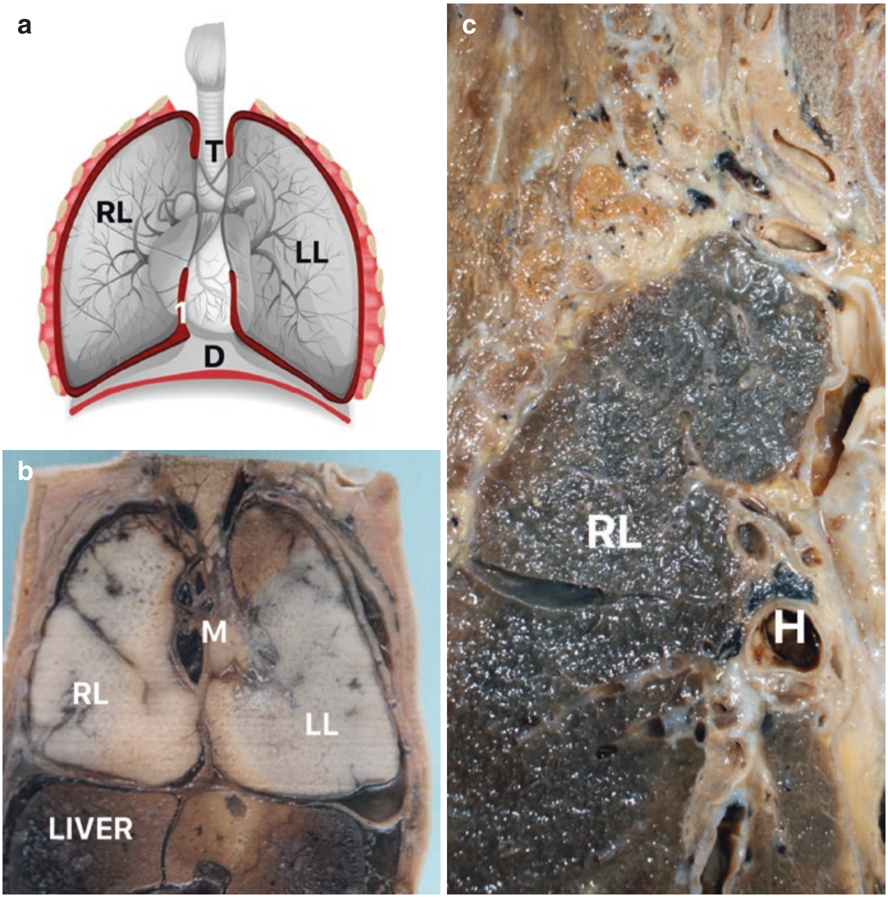

Fig. 1.7 Pleura and pulmonary apex. (**a**) Schematic drawing showing the pleura (1 and all red line) distribution in the thoracic cavity; D, diaphragm; T, trachea; RL, right lung; LL, left lung. (**b**) The figure shows a frontal section of a frozen human fetus in the second gestational trimester; we can oberve the relationships of the mediastinum (M) with the lungs (RL, right lung; LL, left lung). (**c**) Frontal section of a human frozen corpus showing the relationships of the right pulmonary apex; RL, right lung; H, pulmonary hilum

Approximately in the middle of this face is the pulmonary hilum, which is the region where bronchi, vessels, and nerves enter and leave the lung, forming the pulmonary root (Netter 1978; Williams et al. 1995).

The right lung is shorter than the left due to the elevation of the diaphragm. It is also wider as a consequence of the displacement of the heart to the left. Thus, the right lung is heavier, and its total capacity is greater. It has two fissures: horizontal and oblique, and they separate into three lobes (superior, middle, and inferior). The horizontal fissure separates the superior lobe from the middle lobe, and the oblique fissure separates the inferior lobe from the middle and superior lobes. The middle

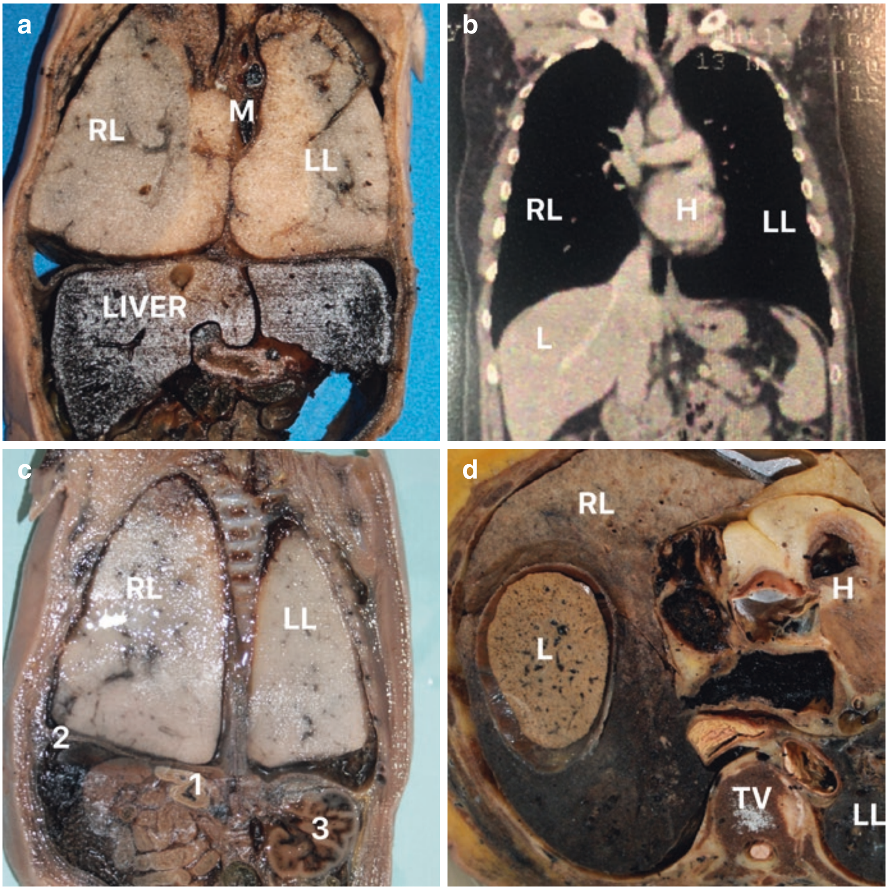

Fig. 1.8 Mediastinum and lungs. (**a**) The figure shows a frontal section of a frozen human fetus in the second gestational trimester; we can oberve the relationships of the mediastinum (M) with the lungs (RL, right lung; LL, left lung). (**b**) The figure shows a thoracic computerized tomography in frontal section; we can observe the heart (H), the right lung (RL), the left lung (LL), and the liver. (**c**) The figure shows a posterior frontal section of a frozen human fetus in the second gestational trimester; we can oberve the lungs (RL, right lung; LL, left lung), the right suprarenal gland (1), the diaphragm (2), and the left kidney (3). (**d**) The figure shows an inferior view of a transverse section of a frozen fresh corpus at the level of the ninth thoracic vertebra (TV); we can observe the heart (H), the lungs (RL, right lung; LL, left lung), and the liver (L)

lobe is wedge-shaped, as it is limited superiorly by the horizontal fissure that is at the level of the fourth costal cartilage and bumps into the oblique fissure in the midaxillary line (Williams et al. 1995).

The left lung has only the oblique fissure, which separates into two lobes: superior and inferior. The lower part of the superior lobe forms an extension between the oblique fissure and the cardiac notch, which is called the lingula, that corresponds to the middle lobe of the right lung.

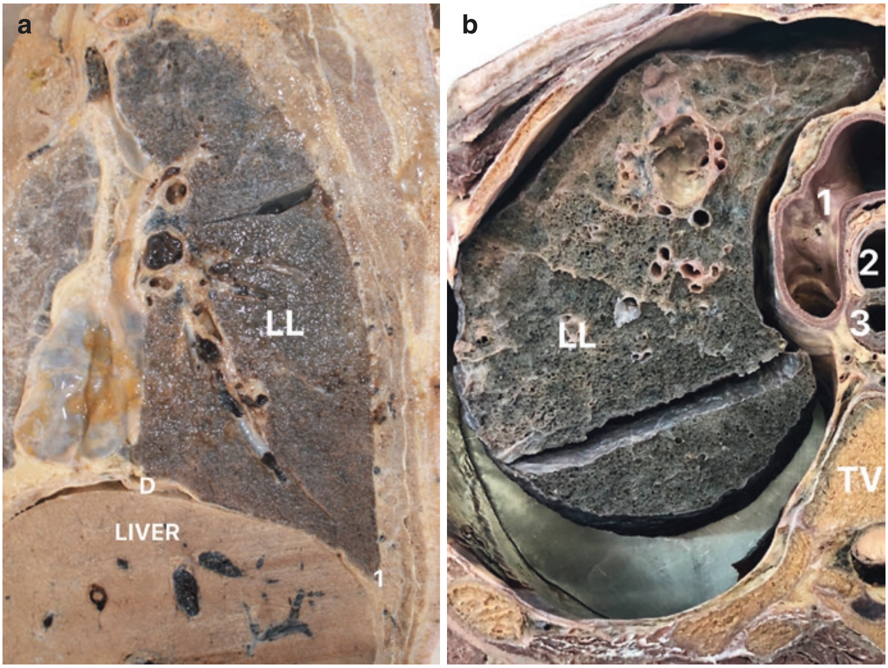

Fig. 1.9 Lungs. (**a**) Frontal section of a human frozen corpus showing the relationships of the left lung (LL) with the diaphragm (D); we can also observe the costophrenic recess (1). (**b**) The figure shows a transverse section of the thoracic cavity of a frozen corpus at the level of the fourth thoracic vertebra (TV); we can observe the left lung (LL), the aortic arch (2), the trachea (2), and the esophagus (3)

1.4.2.1 Bronchopulmonary Segments

Each lobe is divided internally into smaller parts called bronchopulmonary segments. The lung is formed by the union of all bronchial branches; thus, the bronchopulmonary segment is the portion of the lung where a particular bronchus is distributed. The pulmonary segments are the anatomical, functional, and surgical units of the lungs. They are formed by the bronchial tree that begins in the trachea that divides into two main (pulmonary) bronchi. These are divided into three secondary (lobar) bronchi on the right and two on the left, each one for a lobe of the lungs. Finally, the secondary bronchi are divided into tertiary (segmental) bronchi for the pulmonary segments. Knowledge of the lung segment system is essential for understanding human anatomy and has great clinical relevance (Netter 1978). The distribution of the end-branch generation among the five lobes is significantly different. The median branching generation value in the right middle lobe is significantly low compared with that of the other four lobes, whereas that of the right inferior lobe is significantly larger than that of both the right and left superior lobes (Cai et al. 2020; Fujii et al. 2020).

A bronchopulmonary segment is the largest division of the pulmonary lobe. It has a pyramidal shape, with the apex pointing to the pulmonary root and the base facing the costal surface, and it is separated from adjacent segments by septa of connective tissue. It has its own supply through a tertiary bronchus and a segmental artery, which is a tertiary branch of the pulmonary artery and can be surgically removed without affecting the anatomy of nearby segments. The drainage of the bronchopulmonary segment is made by intersegmental veins that drain through the connective tissue that separates one segment from the other. Thus, venous drainage does not respect segmentation, as a vein drains adjacent segments (Netter 1978).

Each tertiary bronchus divides into approximately 20 terminal bronchioles that branch into respiratory bronchioles. These, again, are divided into alveolar ducts, which end in the pulmonary alveoli. The alveolus is the structural unit where the gas exchange takes place.

The bronchopulmonary segments are named according to their position in the lobes. The superior lobe of the right lung has three segments: one apical, one posterior, and one anterior. The right middle lobe has two segments: the lateral and the medial. The inferior lobe of the right lung has five segments: the upper segment and four basilar segments (the medial, anterior, lateral, and posterior basilar segments). The left lung has two segments in the upper part of the superior lobe, the apico-posterior and the anterior, and in the lingula two more segments called the superior lingular and the inferior lingular segments. In the inferior lobe of the left lung, there are the upper segment and three basilar segments, the anteromedial basal, the lateral basal, and the posterior basal (Williams et al. 1995).

Arterial irrigation of the lungs is done by the pulmonary arteries that take blood (venous) to be oxygenated and by the bronchial arteries that irrigate with nonrespiratory parts such as the larger caliber bronchi and the pulmonary support tissue with oxygenated blood. The pulmonary arteries are branches of the pulmonary trunk that branch into two pulmonary arteries, one pulmonary artery for each lung, that enter the pulmonary hiluses and branch out following the division of the bronchi (Saha and Srimani 2019). The left bronchial arteries are branches of the thoracic aorta, and those on the right are branches of the upper posterior intercostal arteries or a left upper bronchial artery (Williams et al. 1995).

The pulmonary veins, two for each lung, drain (arterial) blood from the lungs to the heart. Venous drainage begins in the pulmonary capillaries, with the joining of smaller veins that drain in the intersegmental septa to larger veins. The venous drainage is of the intersegmental type and does not accompany the arterial or bronchial branching. An intersegmental vein drains adjacent segments.

Pulmonary lymphatic drainage is performed by deep lymphatic vessels and superficial lymphatic drainage by subpleural vessels. Superficial drainage is launched in the deep vessels that accompany the bronchi and pulmonary vessels, towards the pulmonary hilum. The final route is made to the tracheobronchial lymph nodes on the same side. Sometimes the inferior lobe of the left lung drains into the lower tracheobronchial lymph nodes on the opposite side (Fig. 1.7).

In Figs. 1.10, 1.11, 1.12, and 1.13, we show a sequence of sectional sections of the chest showing the main structures that can be visualized.

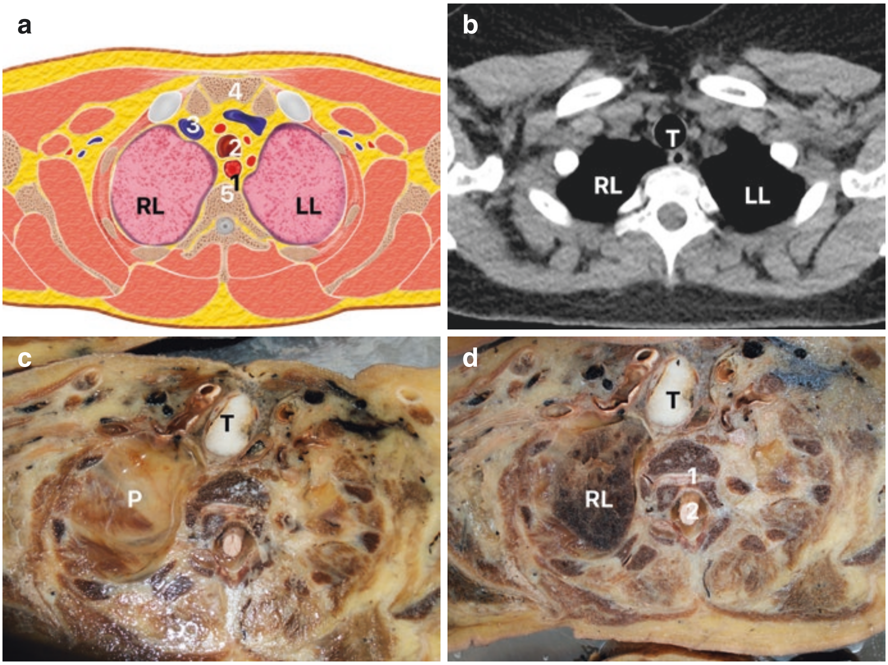

Fig. 1.10 Thoracic sectional anatomy. (**a**) The figure shows a schematic drawing of an inferior view of the thoracic cavity transverse section at the level of the second thoracic vertebra (5); we can observe the right lung (RL), the left lung (LL), esophagus (1), trachea (2), superior vena cava (3), and manubrium of the sternum. (**b**) The figure shows a thoracic computerized tomography in a transverse section at the level of the second thoracic vertebra; we can observe the left lung (LL), right lung (RL), and the trachea (T). (**c**) The figure shows an inferior view of a transverse section of a frozen fresh corpus, at the level of the first thoracic vertebra (TV); we can observe the right pleural cupula (P) and the trachea (T). (**d**) The figure shows an inferior view of a transverse section of a frozen fresh corpus, at the level of the second thoracic vertebra (1); we can observe the right lung (RL) and the trachea (T)

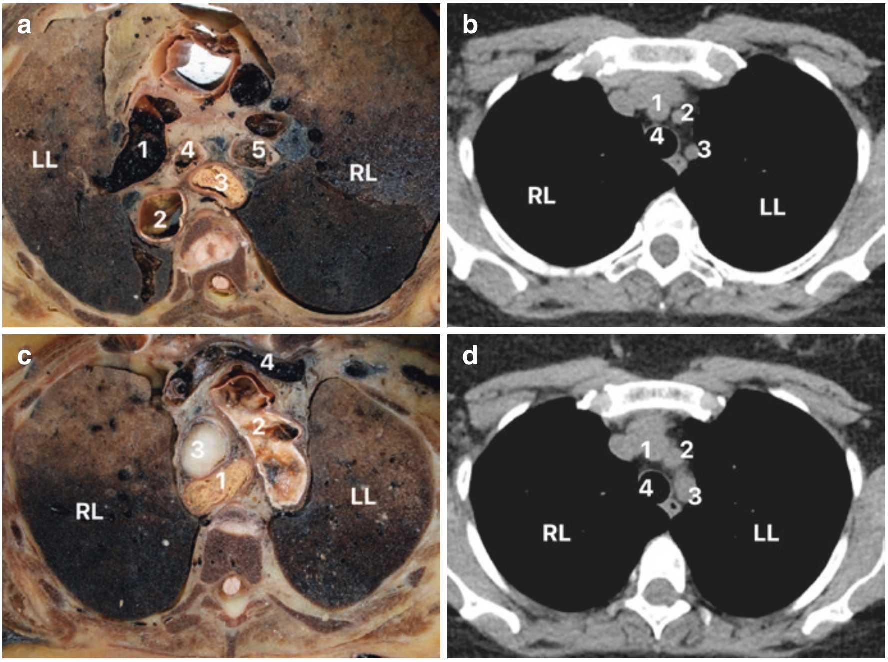

Fig. 1.11 Thoracic sectional anatomy. (**a**) The figure shows a superior view of a transverse section of a frozen fresh corpus, at the level of the fourth thoracic vertebra; we can observe the right lung (RL), the left lung (LL), the left pulmonary artery (1), thoracic aorta artery (2), esophagus (3), left bronchus (4), and right bronchus (5). (**b**) The figure shows a thoracic computerized tomography in a transverse section at the level of the second thoracic vertebra; we can observe the left lung (LL), right lung (RL), the brachiocephalic artery (1), common carotid artery (2), and subclavian artery (3) and trachea (4). (**c**) The figure shows an inferior view of a transverse section of a frozen fresh corpus, at the level of the third thoracic vertebra; we can observe the right lung (RL), the left lung (LL), esophagus (1), aortic arch (2), trachea (3), and the left brachiocephalic vein (4). (**d**) The figure shows a thoracic computerized tomography in a transverse section at the level of the third thoracic vertebra; we can observe the left lung (LL), right lung (RL), the brachiocephalic artery (1), common carotid artery (2), and subclavian artery (3) and trachea (4)

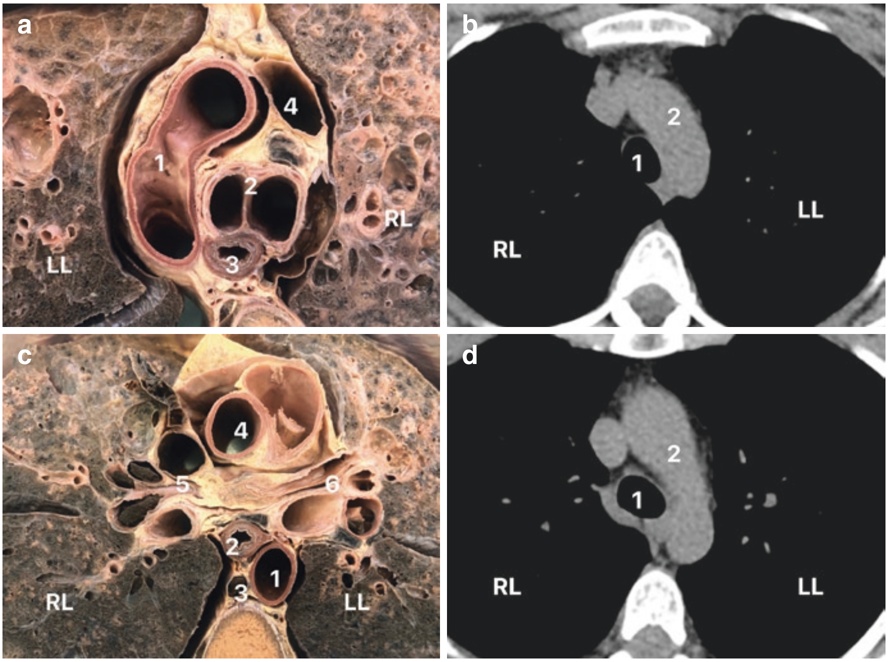

Fig. 1.12 Thoracic sectional anatomy. (**a**) The figure shows a superior view of a transverse section of a frozen fresh corpus, at the level of the fourth thoracic vertebra; we can observe the right lung (RL), the left lung (LL), aortic arch (1), tracheal bifurcation (2), esophagus (3), and pulmonary artery (4). (**b**) The figure shows a thoracic computerized tomography in a transverse section at the level of the transition between the third and fourth thoracic vertebra; we can observe the left lung (LL), right lung (RL), trachea (1), and aortic arch (2). (**c**) The figure shows an inferior view of a transverse section of a frozen fresh corpus, at the level of the transition between the fourth and the fifth thoracic vertebra; we can observe the right lung (RL), the left lung (LL), thoracic aorta artery (1), esophagus (2), azygos vein (3), pulmonary trunk (4), right pulmonary hilum (5), and left pulmonary hilum (6). (**d**) The figure shows a thoracic computerized tomography in a transverse section at the level of the transition between the third and fourth thoracic vertebra; we can observe the left lung (LL), right lung (RL), trachea (1), and aortic arch (2)

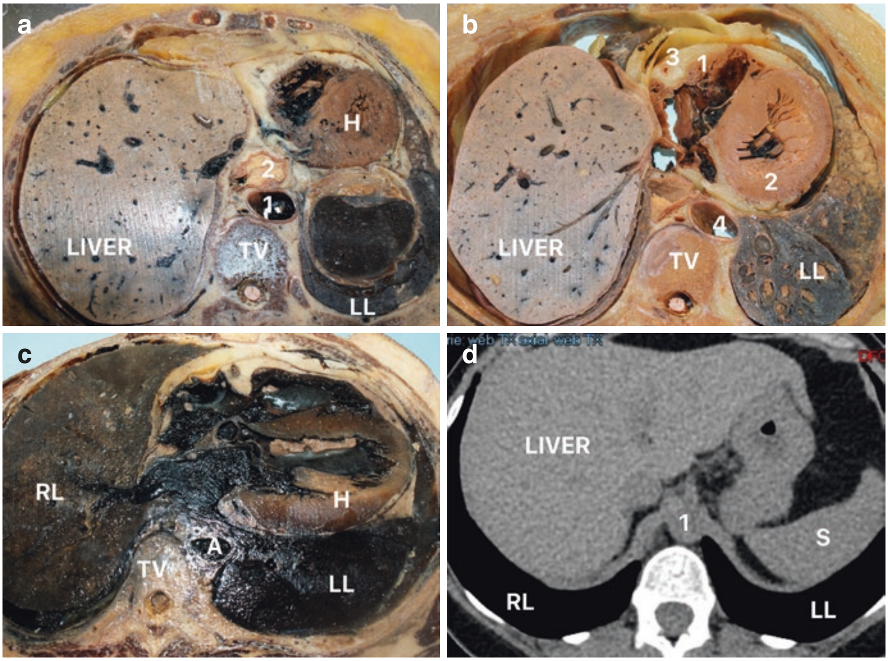

Fig. 1.13 Thoracic sectional anatomy. (**a**) The figure shows an inferior view of a transverse section of a frozen fresh corpus, at the level of the ninth thoracic vertebra (TV); we can observe the liver, the left lung (LL), the heart (H), thoracic aorta artery (1), and esophagus (2). (**b**) The figure shows an inferior view of a transverse section of a frozen fresh corpus, at the level of the eighth thoracic vertebra (TV); we can observe the liver, the left lung (LL), the right ventricle (1), the left ventricle (2), the coronary artery (3), and the thoracic aorta artery (4). (**c**) The figure shows an inferior view of a transverse section of a frozen fresh corpus, at the level of the seventh thoracic vertebra (TV); we can observe the right lung (RL), the left lung (LL), thoracic aorta artery (A), and the heart (H). (**d**) The figure shows a thoracic computerized tomography in a transverse section at the level of the tenth thoracic vertebra; we can observe the left lung (LL), right lung (RL), aorta artery (1), and the spleen (S)

References

Bergman RA, Thompson SA, Afifi AK, Saadeh FA. Compendium of human anatomic variation: catalog, atlas and world literature. Baltimore: Urban & Schwarzenberg; 1988.

Cai P, You Y, Jin ZW, et al. Three-dimensional analysis of the segmental arrangement of lower lung lobes in human fetuses: is this arrangement a miniature version of adult morphology? J Anat. 2020;236(6):1021–34.

Fujii S, Muranaka T, Matsubayashi J, et al. The bronchial tree of the human embryo: an analysis of variations in the bronchial segments. J Anat. 2020;237(2):311–22.

Fujiwara H, Kanamori J, Nakahima Y, et al. An anatomical hypothesis: a "concentric-structured model" for the theoretical understanding of the surgical anatomy in the upper mediastinum required for esophagectomy with radical mediastinal lymph node dissection. Dis Esophagus. 2019;32(8):doy119.

Koutsoufianiotis K, Daniil G, Paraskevas G, et al. Computed tomography angiography study of the azygos vein course and termination into superior vena cava: gender and age impact. Surg Radiol Anat. 2021;43(3):353–61.
Moghari MH, Geest RJ, Brighenti M, Powell AJ. Cardiac magnetic resonance using fused 3D cine and 4D flow sequences: validation of ventricular and blood flow measurements. Magn Reson Imaging. 2020;74:203–12.
Mouchova Z, Rosova B, Matej R. Frozen section of lung, pleura and mediastinum specimen: retrospective analysis of 5-years practical experiences and review of the literature. Cesk Patol. 2018;54(3):127–31.
Nakazono T, Yamaguchi K, Egashira R, et al. CT-based mediastinal compartment classifications and differential diagnosis of mediastinal tumors. Jpn J Radiol. 2019;37(2):117–34.
Netter F. Heart, vol. 2. New Jersey: Ciba; 1978.
Saha A, Srimani P. Comprehensive study of pulmonary hilam with its clinical correlation. Ann Anat. 2019;222:61–9.
Testut L, Jacob O. Anatomia Topográfica. Tomo I. Barcelona: Salvat; 1926. p. 643–781.
Williams PL, Bannister LH, Berry MM, Dyson M, Dussek JE, Ferguson MWJ. In Gray's anatomy. 38th ed. Churchill-Livingstone: Edinburgh; 1995.